Graduate Research in Engineering and Technology (GRET)

Volume 1
Issue 4 *Emerging Aerospace Technologies in Aerodynamics, Propulsion, and Materials.*

Article 2

January 2022

Finite Element Study on the Effect of Geometrical Parameters on the Mechanical Behavior of 3D Reentrant Auxetic Honeycombs.

Sai Adithya Vanga
Institute of Aeronautical Engineering, Dundigal, Hyderabad, adithya.vanga8@gmail.com

Aravind Rajan Ayagara
Institute of Aeronautical Engineering, Dundigal, Hyderabad, a.rajan@iare.ac.in

Rohan Gooty
Institute of Aeronautical Engineering, Dundigal, Hyderabad, g.rohan@iare.ac.in

Taha Hussain
Institute of Aeronautical Engineering, Dundigal, Hyderabad, taha.hussain583@gmail.com

Moulshree Srivastava
Institute of Aeronautical Engineering, Dundigal, Hyderabad, moulshree18@gmail.com

Recommended Citation

Vanga, Sai Adithya; Ayagara, Aravind Rajan; Gooty, Rohan; Hussain, Taha; and Srivastava, Moulshree (2022) "Finite Element Study on the Effect of Geometrical Parameters on the Mechanical Behavior of 3D Reentrant Auxetic Honeycombs.," *Graduate Research in Engineering and Technology (GRET)*: Vol. 1 : Iss. 4 , Article 2.
DOI: 10.47893/GRET.2022.1043
Available at: https://www.interscience.in/gret/vol1/iss4/2

Finite Element Study on the Effect of Geometrical Parameters on the Mechanical Behavior of 3D Reentrant Auxetic Honeycombs

V Sai Adithya, Dr. Aravind Rajan Ayagara, Rohan Gooty, Moulshree Srivatsava, Taha Hussain

1 Abstract-

Auxetic materials are a special case of cellular materials, which exhibit a negative Poisson's ratio. This in fact is the reason behind their peculiar behavior *i.e.* lateral shrinkage under longitudinal compression and vice versa. Since these materials do not obey the laws of "normal" materials and go beyond common sense, they are still an emerging class which can be put to use for various purposes like self-locking reinforcing fibers in composites, controlled release media, self-healing films, piezoelectric sensors, and also be used in biomedical engineering. Their stress-strain behavior, Poisson's ratio and impact energy absorption are controlled by bulk material as well as the unit cell geometry. Among many forms of auxetic structures available, we have chosen a three-dimensional reentrant auxetic honeycomb unit cell. The unit cell geometrical parameters were taken from literature. In this study, we try to understand the effects of strut angle through finite element simulations while keeping the bulk material, unit cell size, strut thickness and number of repetitions constant. A total of three different angles were tested, based on which we conclude that as angle increases, the Poisson's ratio increases and Energy absorption is maximum at 30 deg.

Keywords: Auxetic Material, Poisson's Ratio, Densification, Quasi Static Loading, Deformation mechanism.

2 Introduction

There's so much to selecting the right material like considering the strength, flexibility, weight etc. that many new materials have been developed in an attempt to find the perfect one for the job. One such emerging class of materials is that of the auxetic materials which have a negative poisson's ratio. The word auxetic originates from the word '*auxetos*' in Greek language, which means "*may have increased* ". These materials expand when stretched and decrease in dimension when compressed, defying the basic sense of materials which is thinning when stretched and bulging when compressed. Auxetic materials occur naturally and can be seen in a variety of biological and non-biological materials like salamander skin, cow teat skin, cat skin, single crystals of arsenic and cadmium, α-cristobalite, iron pyrites, etc.

Even though Auxetic meta materials occur in nature, they aren't abundantly found and thus attempts have been made to synthesize them. Auxetic foam was successfully manufactured in 1987 making it the first Auxetic structure to be synthesized. Since then, they have been widely studied

and have applied to different geometrical forms. Today, Auxetic structure exist in the form of foams, 2D structure and 3D structures as well. Auxetic materials are a specific category of cellular materials. Their stress-strain behavior resembles that of a cellular material (as in Fig 1). It consists of three distinct phases, (i) linear elastic phase till yield point, followed by (ii) plateau state with constant stress for increasing strain, and (iii) densification phase *i.e.* exponential increase in stress for slight increase in strain.

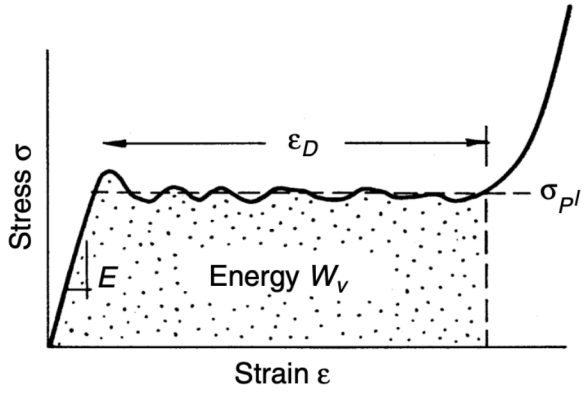

Figure 1 Stress strain behavior of a cellular material.

When cellular materials or Auxetic structures are subjected to loads, some unit cells buckle whilst other stay intact. This means that the sample can undergo further deformation, keeping stress levels constant (Figure 1). Once almost all unit cells undergo plastic buckling, the sample is so weak that even a slight increase in strain will cause an exponential increase in stress (Figure 1) Even though sample still deforms after the point of densification, it shall be of no use. Thus, we evaluate Auxetic structures during its linear elastic phase and plateau phase. In simpler terms, the area of the stress strain curve from 0% strain to densification strain ε_d gives us the energy absorbed during its deformation.

It is aforementioned, that Auxetic structures are a specific form of cellular materials and thus have void contents as well as solid structures. This is where the variable relative density plays a crucial role. Relative density is the ratio of density of the sample over the density of solid material. It gives an idea on the porosity of the sample. The geometrical parameters such as strut thickness and unit cell length, control the amount of solid bulk material existing in the sample. Unit cell of a 3D reentrant Auxetic honeycomb[1] is presented in Fig.2.

The parameters controlling auxetic behavior of 3D reentrant honeycomb were taken from [2]. As per their research work, three parameters control the end result of 3D reentrant honeycomb, strut thickness t, unit cell length a, and the strut angle θ. Strut thickness and unit cell length can be merged one single non-dimensional parameter ζ. Therefore, we have two parameters that decide the required thickness and angle for corresponding relative density. For sake of simplicity and better comprehension, relative density, unit cell length, and thickness were kept constant at 0.16, 10 mm and 1.242 mm respectively.

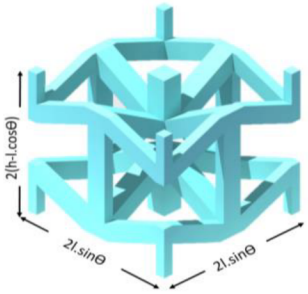

Figure 2 Unit cell of a 3D reentrant honeycomb

3 Numerical simulations

The finite element simulations were carried out on the LS-Dyna explicit solver, which offers numerous contact algorithms between deformable and rigid bodies. The geometries designed in CATIA V5 were imported to ANSYS workbench in the LS Dyna environment to mesh and create the keyword file. The model is subjected to quasi static uniaxial compression. The model is an assembly of a top plate, 3DRAH structure, and a bottom plate. The top and bottom plates were assumed to be rigid structures whereas the 3DRAH is a deformable one (see Fig. 3.). The following paragraphs present the details on the FE model.

The top and bottom rigid plates were considered of $60\text{mm} \times 60\text{mm} \times 3\text{mm}$ and were meshed with 8 node hexahedral elements with one Gaussian integration point [3] (ELFORM = 1). The element size chosen for rigid plates was 1mm to avoid the formation of three-dimensional stress wave in a rigid or elastic .On the other hand, the 3DRAH structure was meshed using tetrahedron elements (ELFORM = 13), which are similar to tetrahedron elements with one integration points but with an additional average of pressure. This additional averaging of nodal pressure, decreases the volumetric locking observed in numerical simulations involving incompressible or ductile materials. The element size chosen for Auxetic sample was $t/2$ *i.e.,* 0.621mm to avoid the formation of volumetric locking as well as negative volume that arises due to large element size in tetrahedral elements.

Boundary conditions are also one of the important aspects for a good and reliable FE model. The experimental test is uniaxial; therefore, the bottom plate is fixed whereas the top plate is given a displacement boundary condition along z axis at a rate of $25\text{mm}\cdot\text{min}^{-1}$ [2]. The Auxetic sample was free to move along all three directions.

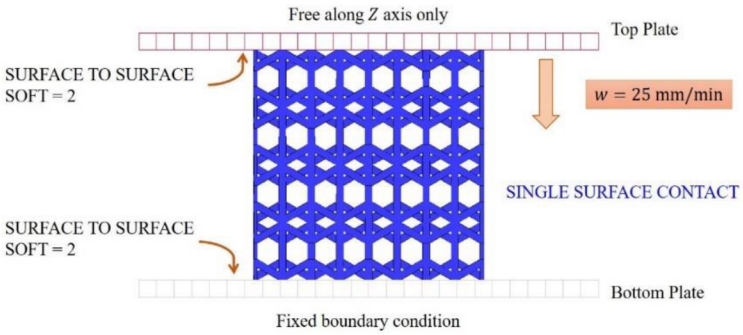

Figure 3 Finite element model of auxetic compression

The loading plates were assumed to be rigid in nature, thus, the material model *MAT-009 RIGID of LS Dyna material library [4] was used to define them, using density 7800 kg·m^{-3}, Young's Modulus of 210GPa and Poisson's Ratio 0.3. The Auxetic structure is made of Poly Lactic Acid (PLA). Auxetic structure was modelled using a Piecewise Elastic Plastic constitutive law (*MAT-024) in the LS Dyna material library. Tension compression tests on PLA coupons were carried out to furnish the constitutive law. The mechanical properties are *MAT-024 PIECEWISE_LINEAR_PLASTICITYof LS Dyna material library was used to define them, using density 1300 kg·m^{-3}, Young's Modulus of 1.743GPa and Poisson's Ratio 0.36. No damage laws were included in the analysis.

Another important aspect of the numerical simulation is the transfer of forces from the rigid plate to Auxetic sample. This is possible by defining an appropriate contact algorithm between the rigid plates and Auxetic sample. Even though the rigid plate moves at a constant speed, in turn applying load on the Auxetic structure, the energy transmission between each constituent of the assembly as well as the transmission of forces between two continuums cannot be done just by giving different properties. There must be a physical contact that shall help the solver to recognize different continuums of the system. For this purpose, a total of three contacts were defined between each constituent of the assembly. An automatic surface to surface contact based on the pinball segment penalty formulation was defined between the Auxetic and the rigid plates (*CONTACT_AUTOMATIC_SURFACE_TO_SURFACE with SOFT= 2 option of LS Dyna). The pinball segment-based penalty formulation i.e., SOFT = 2 was chosen due to the difference in the order of magnitudes of the material properties of plate and Auxetic structure. To avoid the interpenetration of elements of the Auxetic structure along the compression process, a single surface contact was defined between the elements of Auxetic structure (*CONTACT_AUTOMATIC_SINGLE_SURFACE of LS Dyna). It is to be duly noted that all contacts were assumed to be friction less.

4 Results and Discussions

Angle θ	Elastic Modulus E (MPa)	Densification Modulus E_D (MPa)	Platho Stress σ_{pt} (MPa)	Densification strain ε_D (mm/mm)	Energy Absorbed W_v (J)	Poisson's ratio	
						ν_{xz}	ν_{yz}
25º	28.9161	11.7571	1.3363	0.20075	14.3339	-0.3346	-0.6128
30 º	29.2093	36.6996	1.5503	0.1931	16.7643	-0.2465	-0.2471
35 º	24.4556	15.0988	1.3279	0.2096	14.6022	-0.126	-0.15

Table 1 Summary of key points of 3DRAH

4.1 Poissons ratio

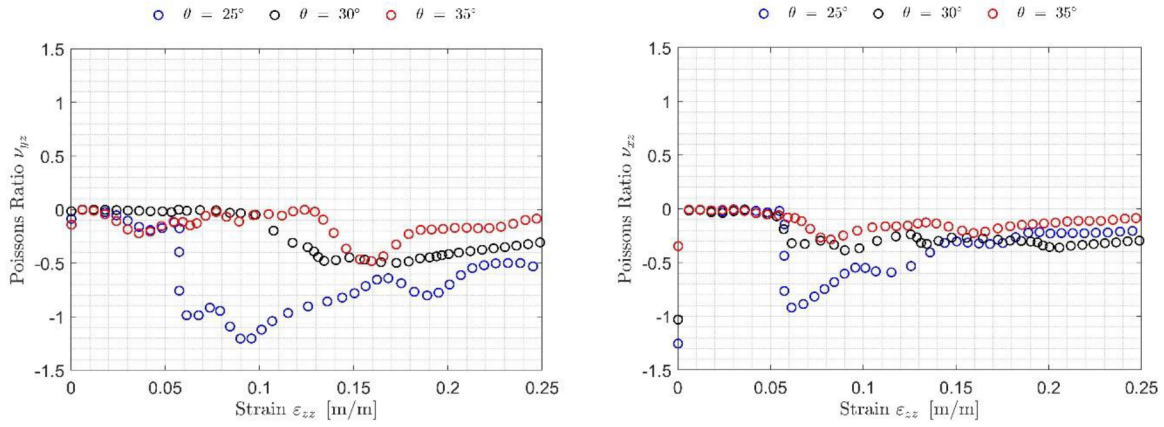

Figure 4

It can be inferred that poissons ratio is increasing with the angle θ, this can be explained by the decrease in the gap between the angular struts in the unit cells with θ, even though the 30^0 sample has greater poissons ratio when compared to 25^0 sample it has more energy absorption capacity which primarily arises from the deformation mechanism of the samples.

4.2 Energy Absorption

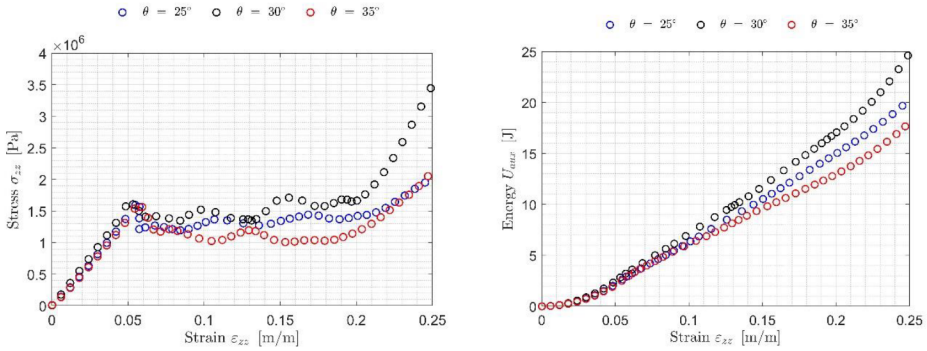

Figure 5 Strain of 3DRAH structure at θ = 25^0, 30^0, 35^0

It has been observed that the 30^0 3DRAH structure has the highest energy absorption and lowest densification strain point with highest Elastic modulus. This can be explained by the deformation mechanism (Figure 6) where very little lateral distortion is observed in the 30^0 sample. It can be deduced that the energy absorption and the magnitude of lateral distortion are inversely proportional.

4.3 Deformation Mechanism

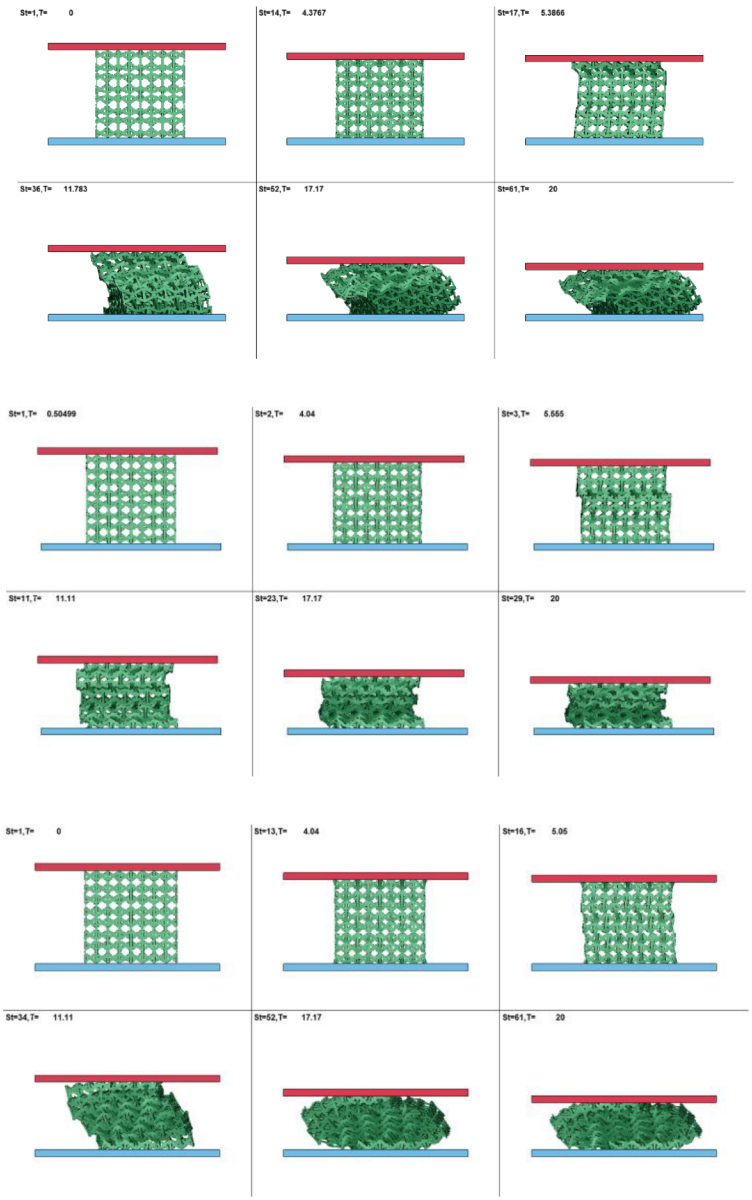

Figure 6 Deformation mechanism of 3DRAH structure at θ=25º, 30º, 35º

It can be absorbed that in 25^0 sample the lateral distortion began at the bottom layer and the buckling starts in the first layer whereas in 35^0 sample the lateral distortion began at the top layer and a uniform buckling is absorbed, this can be explained by the less space between the angular struts in 35^0 3DRAH. The least lateral distortion is observed in the 30^0 sample which

explains the higher energy absorption of the 30^0 sample when compared with 25^0 and 35^0 samples. For example, [5] had presented a wide review but not many articles give an insight on 3DRAH.

5 Conclusion

We have studied the effect of strut angle on 3DRAH through FEM, an automatic surface to surface contact and also automatic single surface contact are most important features in order to transmit forces from one entity to another, the present model predicts that as the angle increases the negative poissons ratio on both directions decreases, whereas the angle has no influence of densification strain yet it had influence on the σ_{pt}, Elastic Modulus and E_D. taking into account of the existing behavior of the deformation mechanism of 3drah we come to a conclusion that an strut angle of 30^0 is giving us an optimized performance. This conclusion of ours is also in accordance with existing literature survery that the strut angle has to be less than 45^0 to avoid interpenetration of struts. For optimum performance under impact energy absorption we suggest the angle should not exceed 30^0.

6 References

[1] D. Faraci, L. Driemeier, and C. Comi, “Bending- Dominated Auxetic Materials for Wearable Protective Devices Against Impact,” *J. Dyn. Behav. Mater.*, Dec. 2020, doi: 10.1007/s40870-020-00284-2.

[2] L. Yang, O. Harrysson, H. West, and D. Cormier, “Mechanical properties of 3D re-entrant honeycomb auxetic structures realized via additive manufacturing,” *Int. J. Solids Struct.*, vol. 69–70, May 2015, doi: 10.1016/j.ijsolstr.2015.05.005.

[3] A. R. Ayagara, A. Langlet, and R. Hambli, “On dynamic behavior of bone: Experimental and numerical study of porcine ribs subjected to impact loads in dynamic three-point bending tests.,” *J. Mech. Behav. Biomed. Mater.*, vol. 98, pp. 336–347, Oct. 2019, doi: 10.1016/j.jmbbm.2019.05.031.

[4] L. S. T. C. (LSTC), *LS DYNAKeyword User ’ S Manual Volume II*, vol. II, no. February. 2012.

[5] G. Lu and Z. You, “Large deformation and energy absorption of additively manufactured auxetic materials and structures: A review,” *Compos. Part B Eng.*, vol. 201, p. 108340, Aug. 2020, doi: 10.1016/j.compositesb.2020.108340.

[6] A. Remennikov, D. Kalubadanage, T. Ngo, P. Mendis, G. Alici, and A. Whittaker, “Development and performance evaluation of large-scale auxetic protective systems for localized impulsive loads,” *Int. J. Prot. Struct.*, vol. 10, pp. 390–417, Sep. 2019, doi: 10.1177/2041419619858087.

[7] M. Alharbi, I. Kong, and V. Patel, “Simulation of uniaxial stress–strain response of 3D-printed polylactic acid by nonlinear finite element analysis,” *Appl. Adhes. Sci.*, vol. 8, Jul. 2020, doi: 10.1186/s40563-020-00128-1.